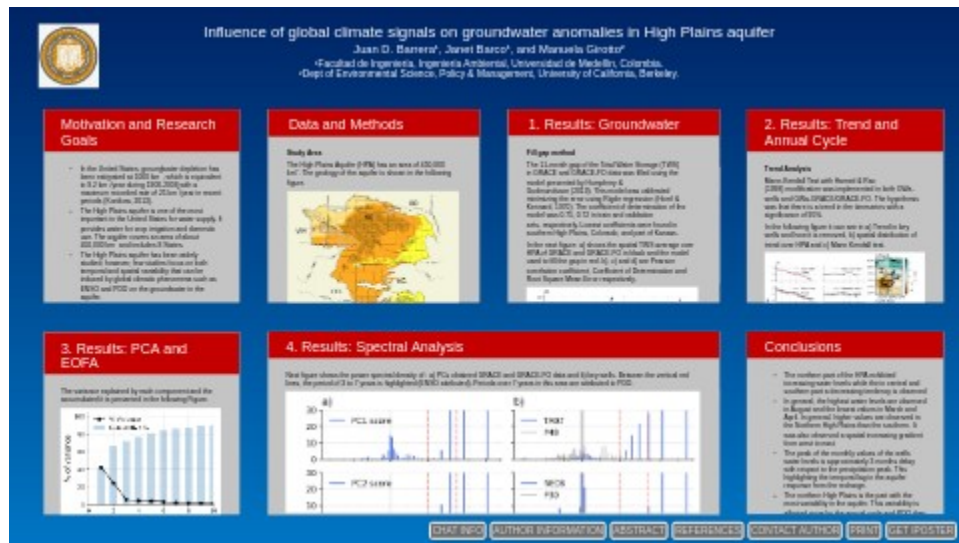


# Influence of global climate signals on groundwater anomalies in High Plains aquifer



Juan D. Barrera<sup>1</sup>, Janet Barco<sup>1</sup>, and Manuela Girotto<sup>2</sup>

<sup>1</sup>Facultad de Ingeniería, Ingeniería Ambiental, Universidad de Medellín, Colombia.

<sup>2</sup>Dept of Environmental Science, Policy & Management, University of California, Berkeley.

PRESENTED AT:



## MOTIVATION AND RESEARCH GOALS

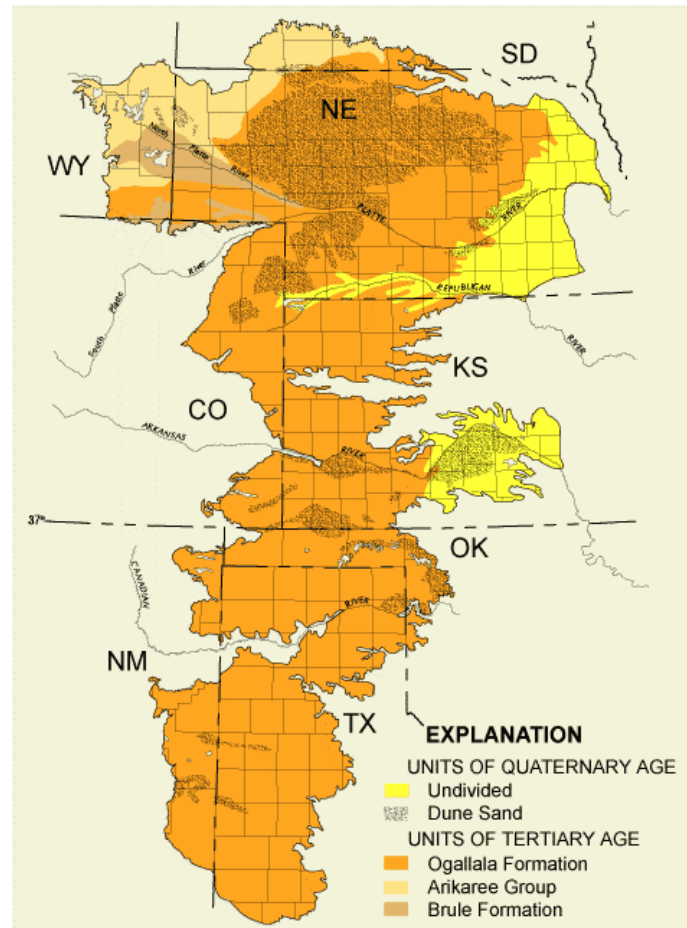
- In the United States, groundwater depletion has been estimated at 1000 km<sup>3</sup>, which is equivalent to 9.2 km<sup>3</sup>/year during 1900-2008 with a maximum recorded rate of 25 km<sup>3</sup>/year in recent periods (Konikow, 2013).
- The High Plains aquifer is one of the most important in the United States for water supply. It provides water for crop irrigation and domestic use. The aquifer covers an area of about 450,000 km<sup>2</sup> and includes 8 States.
- The High Plains aquifer has been widely studied; however, few studies focus on both temporal and spatial variability that can be induced by global climatic phenomena such as ENSO and PDO on the groundwater in the aquifer.

Research Goal: Analyze the influence of global climatic phenomena on groundwater storage in the High Plains aquifer

## DATA AND METHODS

### Study Area

The High Plains Aquifer (HPA) has an area of 450,000 km<sup>2</sup>. The geology of the aquifer is shown in the following figure.



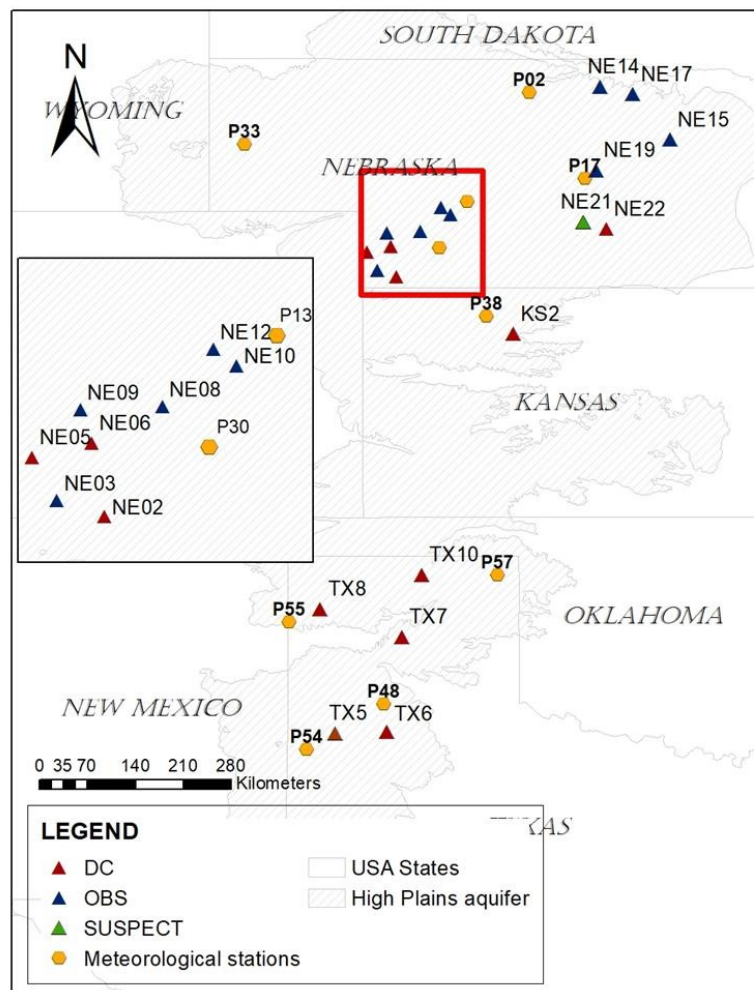
The geological units varies in age from the Permian to the Quaternary. Soils are composed by clay, silt, sand and poorly classified gravel, generally unconsolidated, deposited by streams and wind (Ogallala Formation and Quaternary units), very fine-to-fine grained sandstone (Arikaree Group) and siltstone containing sandstone and interconnected fractures (upper part of Brule Formation) (Gutentag et al., 1984).

**Groundwater (GW)** was extracted from Total Water Storage (TWS) obtained from GRACE and GRACE-FO missions. Soil Moisture (SM) and Snow Water Equivalent (SWE) were obtained from the model North America Land Data Assimilation System (NLDAS). SM and SWE were extracted from TWS. The period of this data is from 2002 to 2020. The groundwater level were obtained from USGS database,

selecting the wells with longer period of records. The selected wells have a period from 1980 to 2020.

Each well data was interpolated with a polynomial and resampled monthly. The well with the longest and most complete period (1948-2020) is KS02 with a percentage of missing data of 9%. This well was used to evaluate the effects of PDO in the aquifer. In addition, data from 10 meteorological stations were obtained from NOAA. This data was used to study changes in groundwater level with changes in precipitation. Wells water levels and precipitation were processed in the same way, with a three months moving average to smooth the time series. The next figure shows wells and precipitation stations locations in High Plains aquifer. Blue wells have not anthropogenic effects. Red wells are affected by pumping, Green well are suspect of being affected by pumping.

## HIGH PLAINS AQUIFER



Two climate indices were used to evaluate the connection between climate and groundwater levels. The Oceanic Niño Index (ONI) that provides thermal anomalies in El-Nino 3.4 was obtained from NOAA Climate Prediction Center. The Pacific Decadal Oscillation (PDO) was also obtained from NOAA.

**Trend** analysis was performed fitting a line in time series and Mann-Kendall Test for significance. The trend was removed for further analysis.

**Principal Component Analysis (PCA) and Empirical Orthogonal Functions Analysis (EOFA)** are statistical methods that allows simplifying the complexity of sample spaces with many dimensions while preserving their information. This method was useful to reduce GW dimensionality obtained from GRACE, GRACE-FO and GLDAS. The method consists of the decomposition of the data of interest into a set of vectors that constitute a linear combination of the original variable and contain most of its variance.

$$Ce = \lambda e$$

Where C is covariance matrix of data, e are eigenvectors and lambda the eigenvalues.

$$PC = eTC$$

Where PC are Principal Components.

The **Spectral Analysis** was carried out with the Fast Fourier Transform (FFT). Using the FFT it is possible to change the signal from time domain to frequency domain and determine the main frequencies of the signal. Here we used Welch's method, which estimate the power spectral density by dividing the data into overlapping segments, computing a modified periodogram for each segment and averaging the periodograms (Welch, 1975) with a Blackman-Harris window (Harris, 1978).

$$x(k) = \sum_{n=0}^{N-1} x(n) e^{-2i\pi kn/N} \quad k=1, 2, \dots, N-1$$

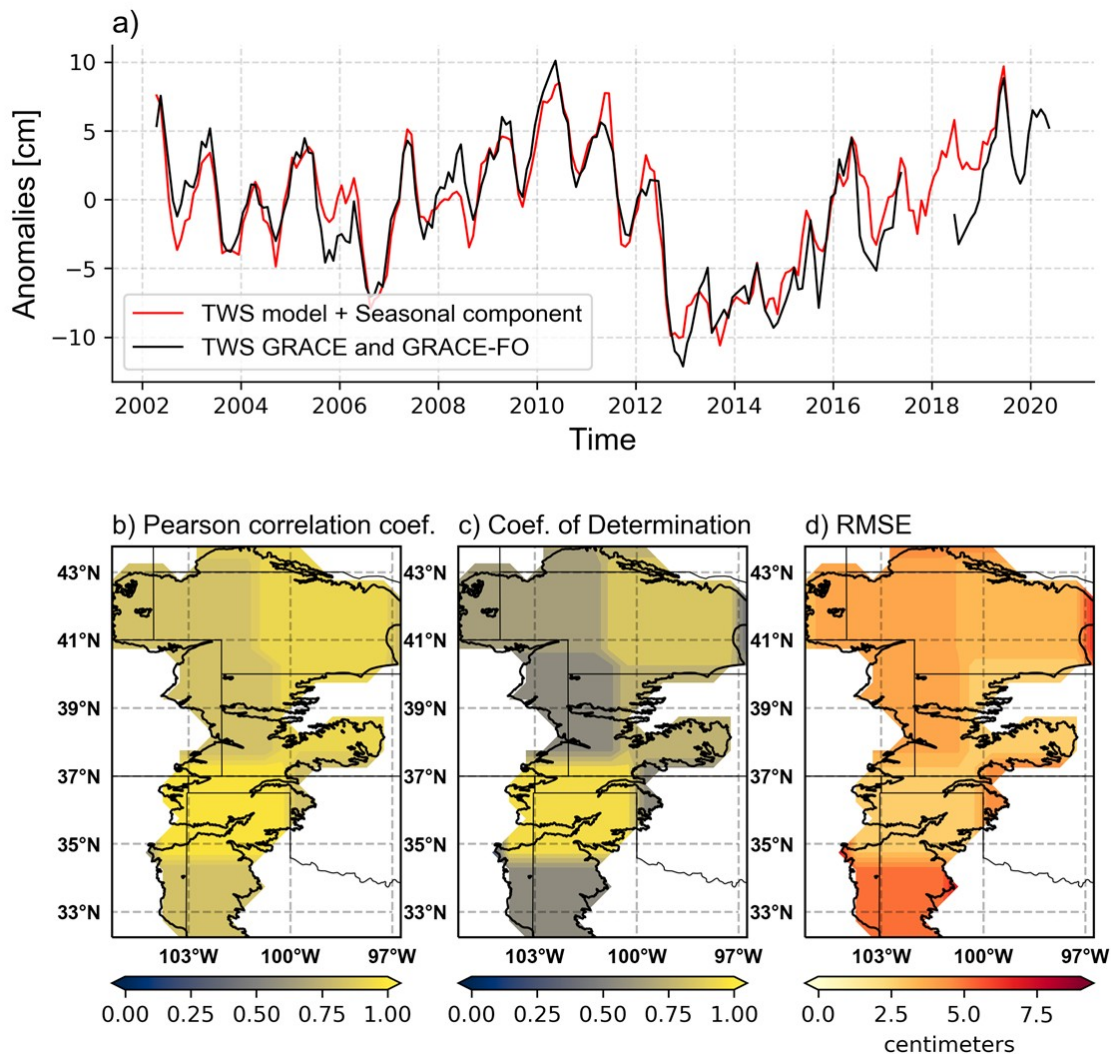
Where x(n) is the periodic signal, k the frequency and N the total number of samples n.

# 1. RESULTS: GROUNDWATER

## Fill gap method

The 11-month gap of the Total Water Storage (TWS) in GRACE and GRACE-FO data was filled using the model presented by Humphrey & Gudmundsson (2019). This model was calibrated minimizing the error using Ridge regression (Hoerl & Kennard, 1970). The coefficient of determination of the model was 0.75, 0.72 in train and validation sets, respectively. Lowest coefficients were found in southern High Plains, Colorado, and part of Kansas.

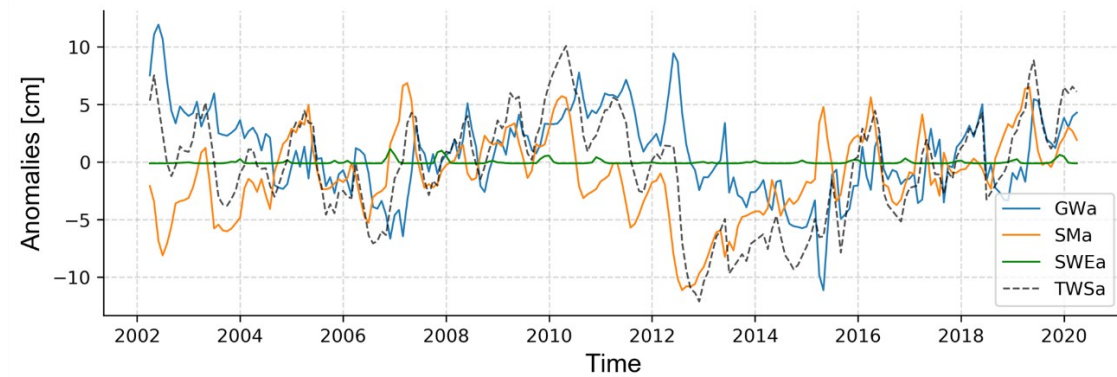
In the next figure: a) shows the spatial TWS average over HPA of GRACE and GRACE-FO in black and the model used to fill the gap in red. b), c) and d) are Pearson correlation coefficient, Coefficient of Determination and Root Square Mean Error respectively.





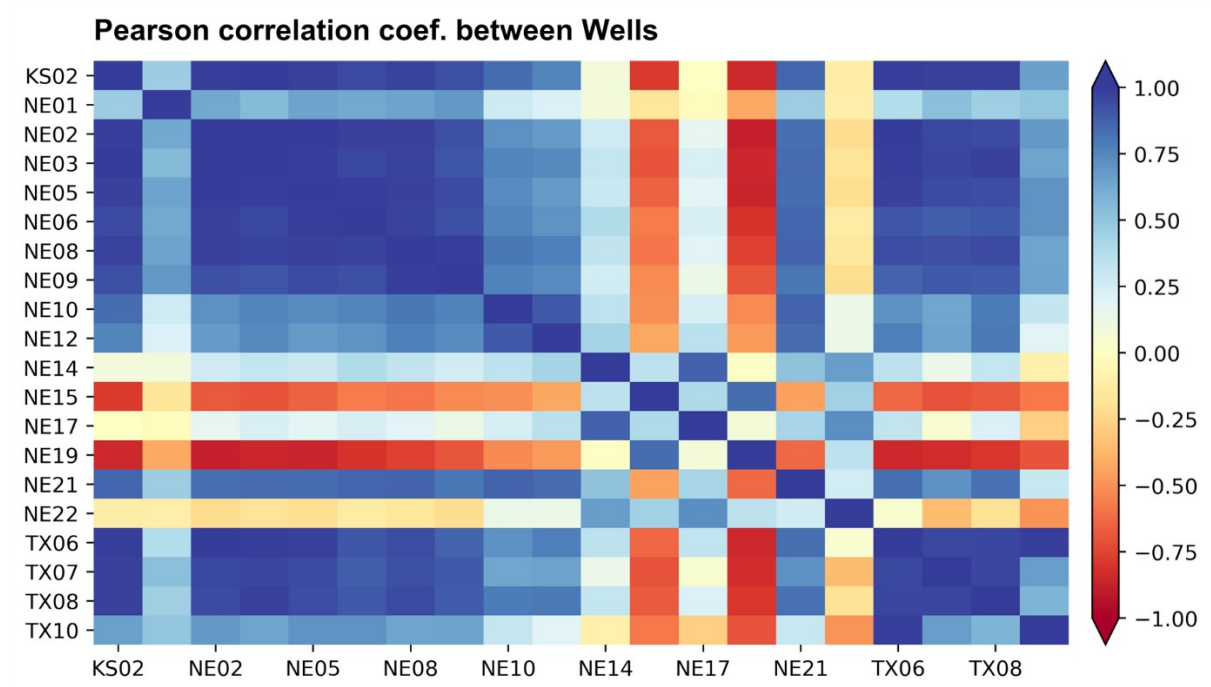
## Groundwater

HPA spatial average of Groundwater anomalies (GWa), Soil Moisture anomalies (SMa), Snow anomalies (SWEa) and TWS anomalies (TWSa) area presented in next figure.



GWa obtained from wells showed different patterns, explaining the variability of the High Plains aquifer. Wells in Texas, Kansas and Nebraska (acronym TX, KS and NE, respectively) seem to have a strong negative trend. It is important to remove those trends before the spectral analysis is performed.

Wells were grouped according to their Pearson correlation in order to select a key well to represents all the wells in each group.



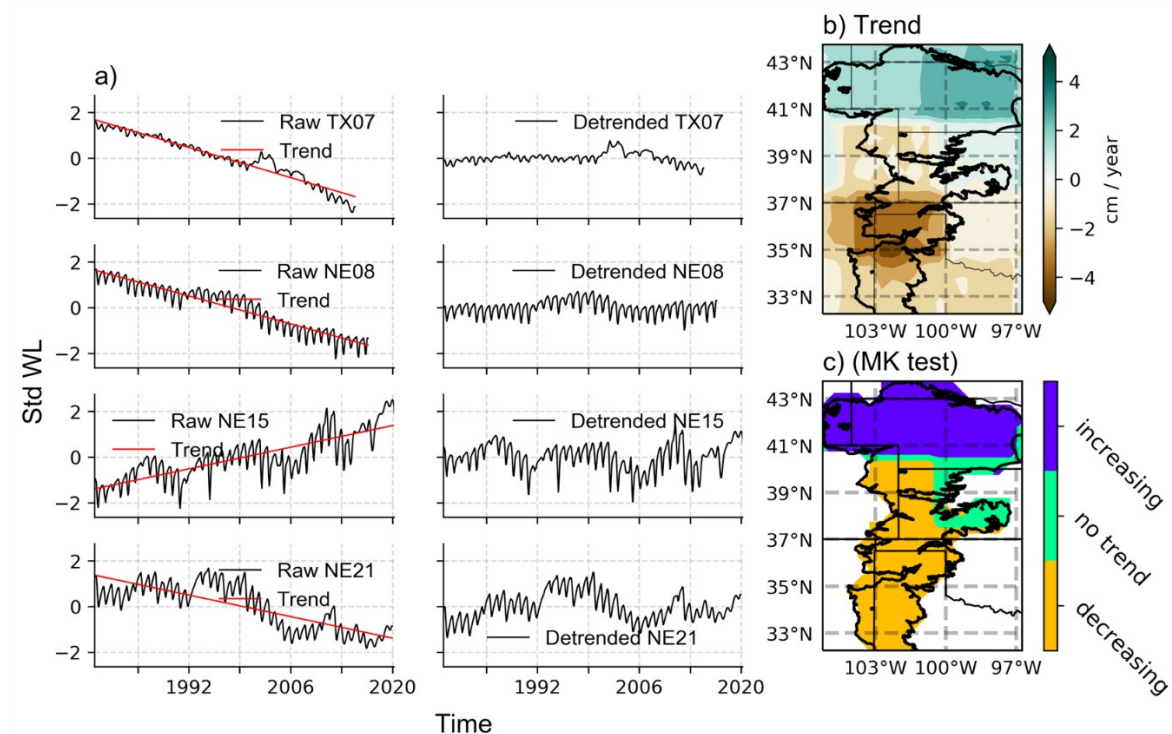
In the previous Figure, it is observed that almost all the wells were positively correlated with each other, except for NE15, NE19 and partially NE22, which had negative correlations with the rest of the wells.

## 2. RESULTS: TREND AND ANNUAL CYCLE

### Trend Analysis

Mann-Kendall Test with Hamed & Rao (1998) modification was implemented in both GWa-wells and GWa-GRACE/GRACE-FO. The hypothesis was that there is a trend in the time series with a significance of 95%.

In the following figure it can see in a) Trend in key wells and how it is removed, b) spatial distribution of trend over HPA and c) Mann Kendall test.



With GWa-GRACE/GRACE-FO, the spatial distribution of the trend was analyzed. Mann-Kendall test detected an increasing trend over the North HPA (Nebraska, South Dakota and Wyoming), no trend was found in part of Nebraska and Kansas and a decreasing trend in the rest of the central and south part of the aquifer. The area with the most level depletion was found between Texas and Oklahoma at 37°N with 4 cm per year while the area with the greatest increase in groundwater was found in eastern Nebraska.

In wells located in Texas, Kansas, and the central part of Nebraska (North Platte and its surroundings) the test detected a negative trend. In NE12, NE14, NE17 and NE22 it was not found trend, while in NE15 and NE19 it was found an increasing trend (wells in zone with highest precipitation, lower altitude, and irrigated zones).

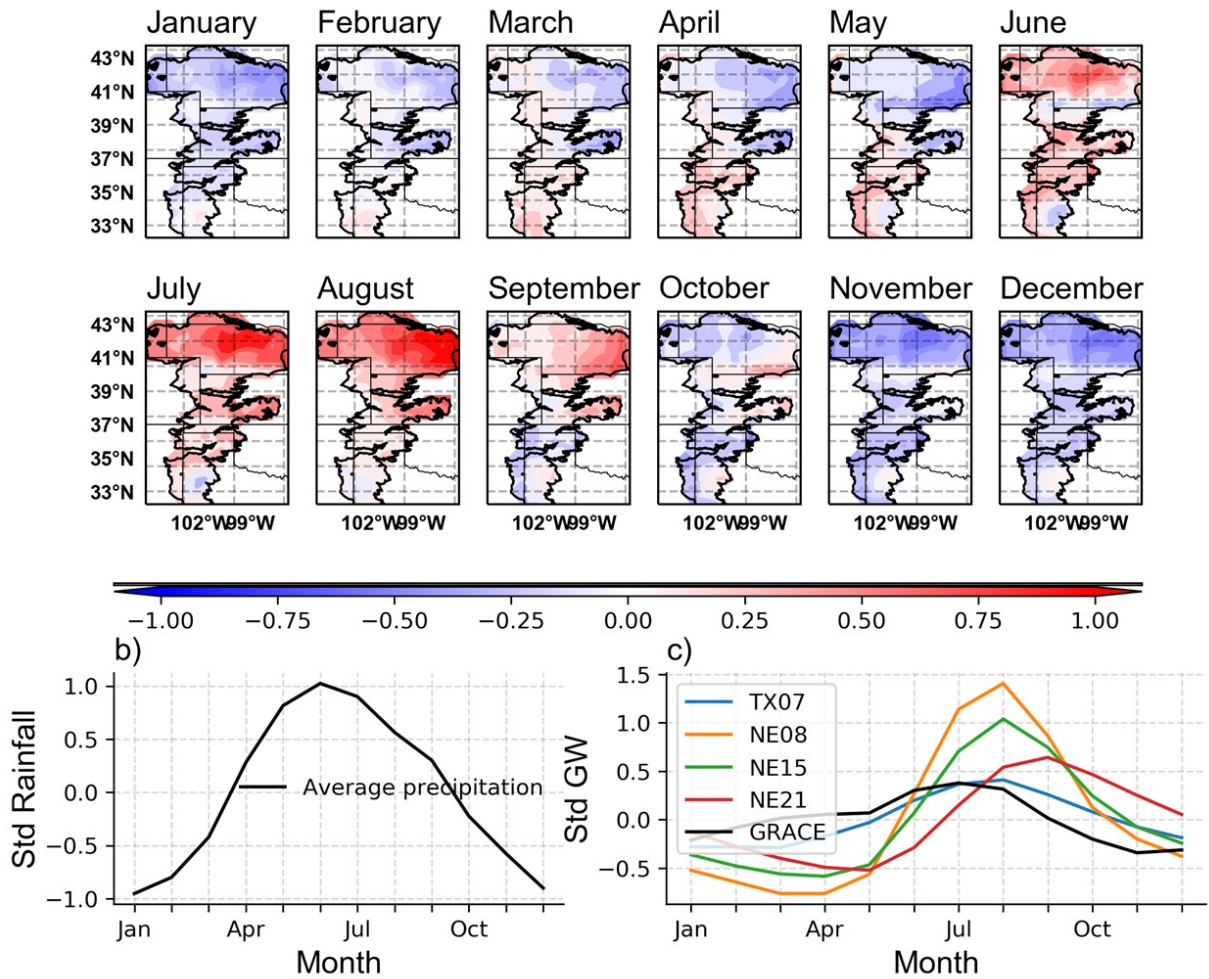
### **Annual Cycle**

In the next Figure is shown the spatial distribution of the standard Annual Cycle of GWa, standard average rainfall Annual Cycle, and standard GWa-wells and GWa-GRACE/GRACE-FO.

Most of the rain falls in May, June, and July while the lowest in December and January. In key wells, the annual cycle had the lowest point at end of winter and beginning of spring, and the peak in July, August and September at summer. In GWa an increasing gradient from west to east is observed. In general, higher values are observed in the Northern High Plains than the southern.

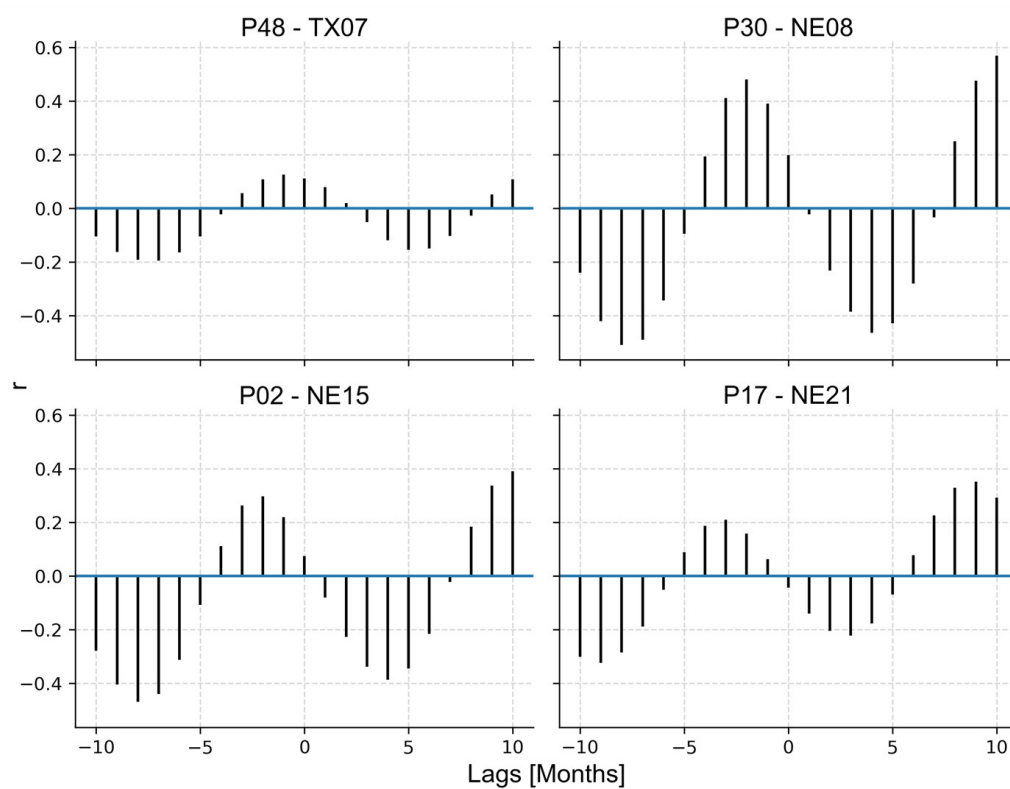


### a) Standard GWa Annual Cycle



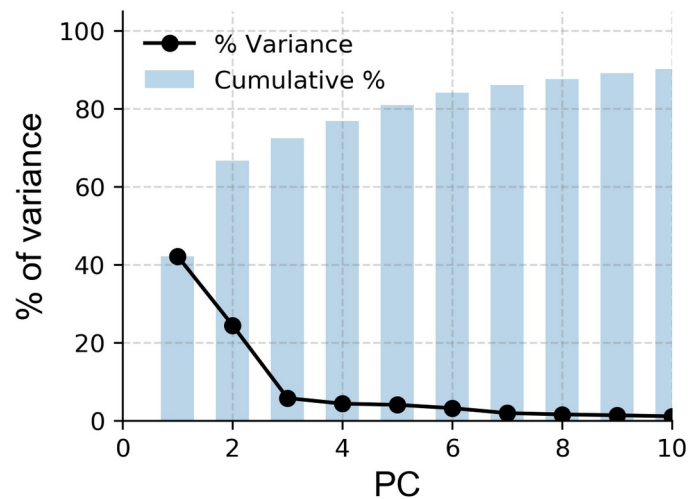
### Lag correlation

In the next figure, it can see the cross correlation between key wells and its nearest precipitation station. The maximum correlation between GWa and precipitation occurs with three or four-month lag.



### 3. RESULTS: PCA AND EOFA

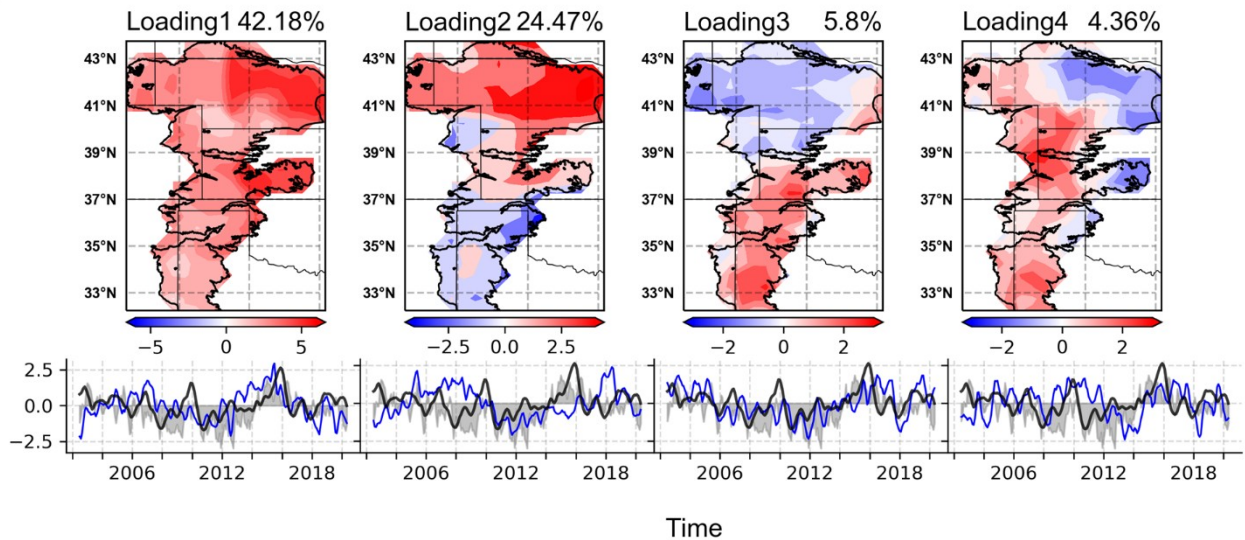
The variance explained by each component and the accumulated it is presented in the following Figure.



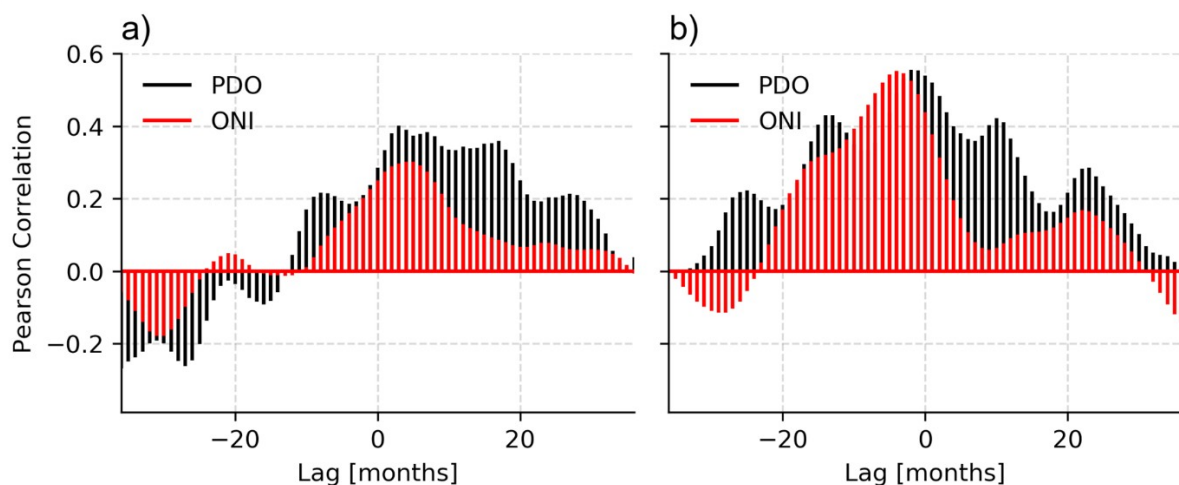
The first component explains 42.2% of the total variance; the second explain 24.5% approximately and the third and fourth explained 5.8% and 4.4% respectively. The 4 PC explained about 77% of the total variance.

The first EOF has more variability in the northeast of the aquifer. It can be explained in terms of the high irrigation in this area; however, this component has positive correlations with ENSO (0.28) and PDO (0.4) indices, with lags of 4 and 3 months, respectively.

The Loadings are Pearson correlations between EOFs and original variables i.e. EOFs scaled by their explained variance. The next Figure shows Loadings of first four EOFs with its respective PC.



The following Figure shows the Cross-correlations the first and third components with the ONI (red) and PDO (black).

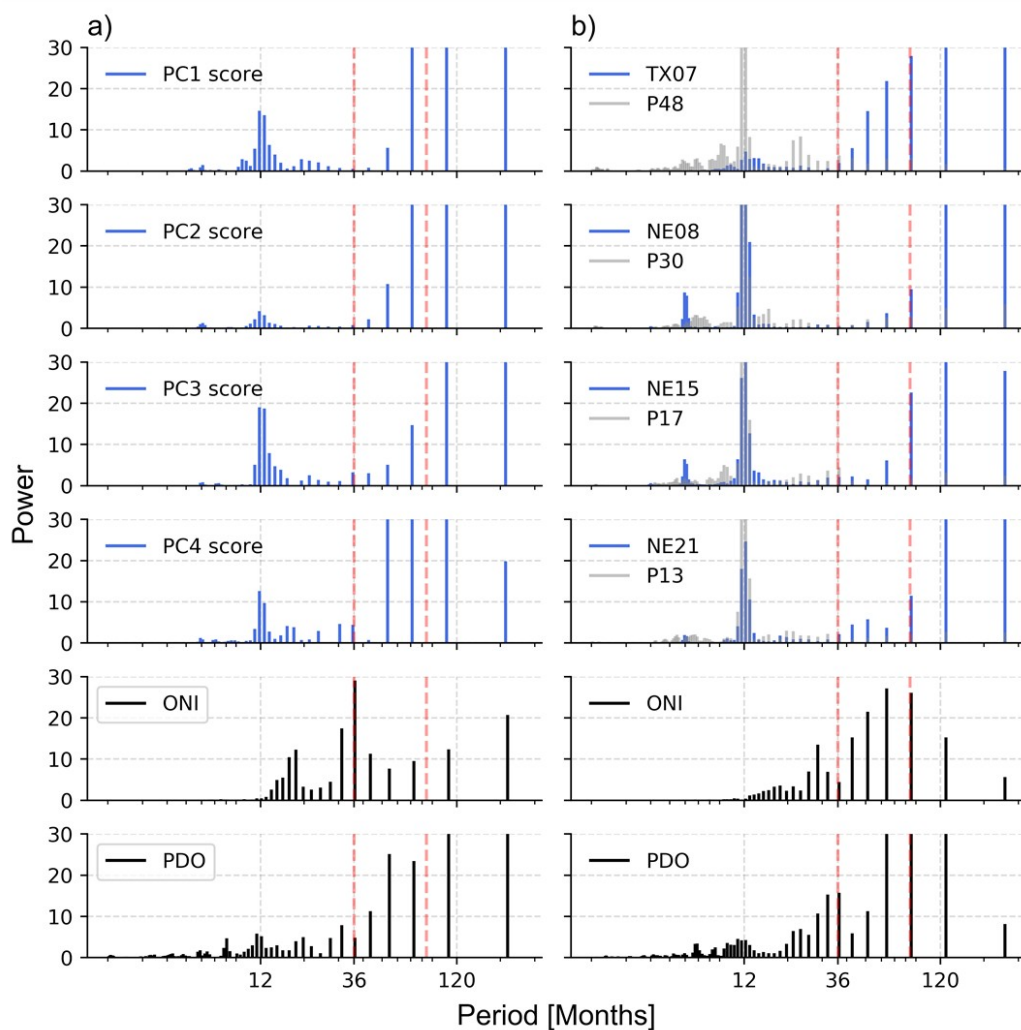


The second EOF followed the variability of the water levels in the aquifer and did not present significant correlations with the indices. The third EOF is the most associated with ENSO and PDO. The Highest correlation occurs when PDO (ONI)

index leads two (four) months the PC. Fourth EOF differentiated the east zone (the most permeable zone of the aquifer by the type of soil) from the high plains. This component did not present significant correlations with the climate indices.

## 4. RESULTS: SPECTRAL ANALYSIS

Next figure shows the power spectral density of : a) PCs obtained GRACE and GRACE-FO data and b) key wells. Between the vertical red lines, the period of 3 to 7 years is highlighted (ENSO attributed). Periods over 7 years in this area are attributed to PDO.

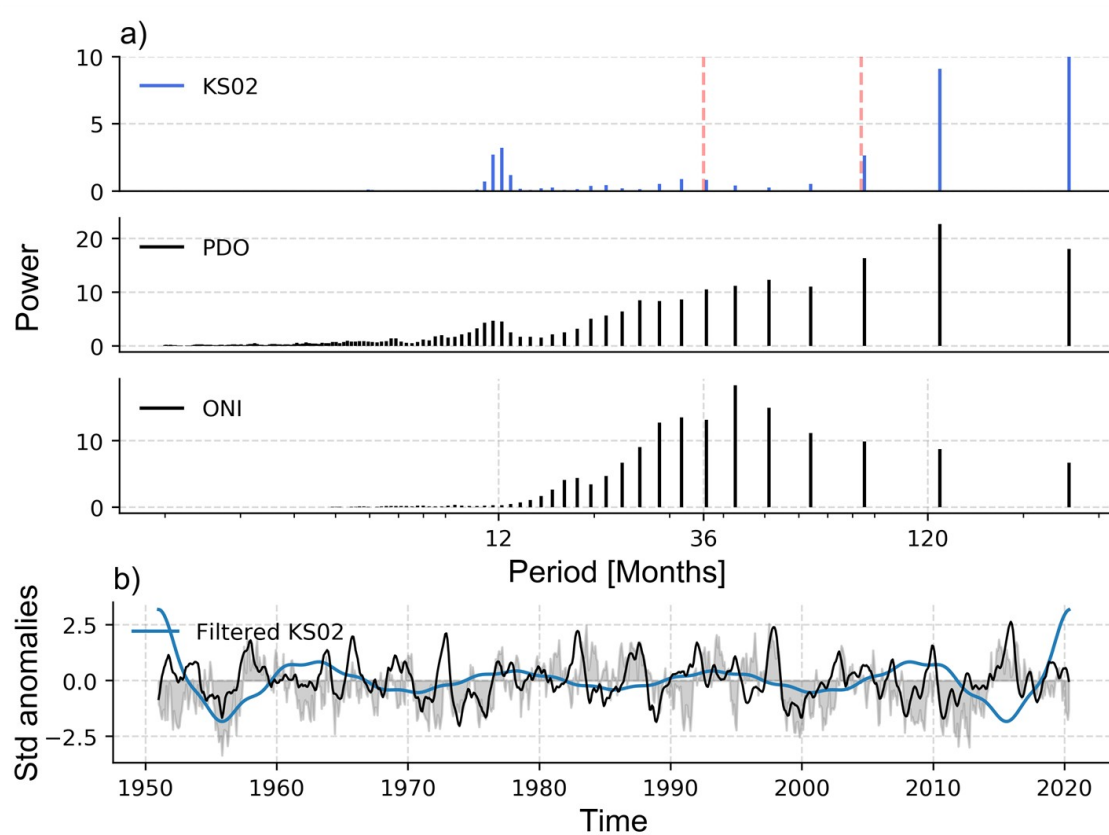


- For a) and b) Spectrum of PDO and ENSO showed similarities with the difference that PDO has dominant low frequencies (> 10 years). The power of frequencies of PDO are stronger than ENSO

- Power spectrum in key wells showed a strong annual cycle in Nebraska wells, while in Texas the seasonality is weaker.
- All wells had variability in the frequencies related with ENSO (NE08 had the lowest power of these frequencies among key wells).
- The first four PCs in GRACE showed a similar behavior to that observed with the wells: annual seasonality and low frequencies associated with ENSO and PDO. However, some differences are expected due to the differences of time series periods between GRACE and well data. The strongest power in ONI is at 3 years, but none of the PC of the water levels had significant variability in this period. Consistent with wells data, PC variability is more affected by the annual cycle and modes related to PDO than to ENSO.

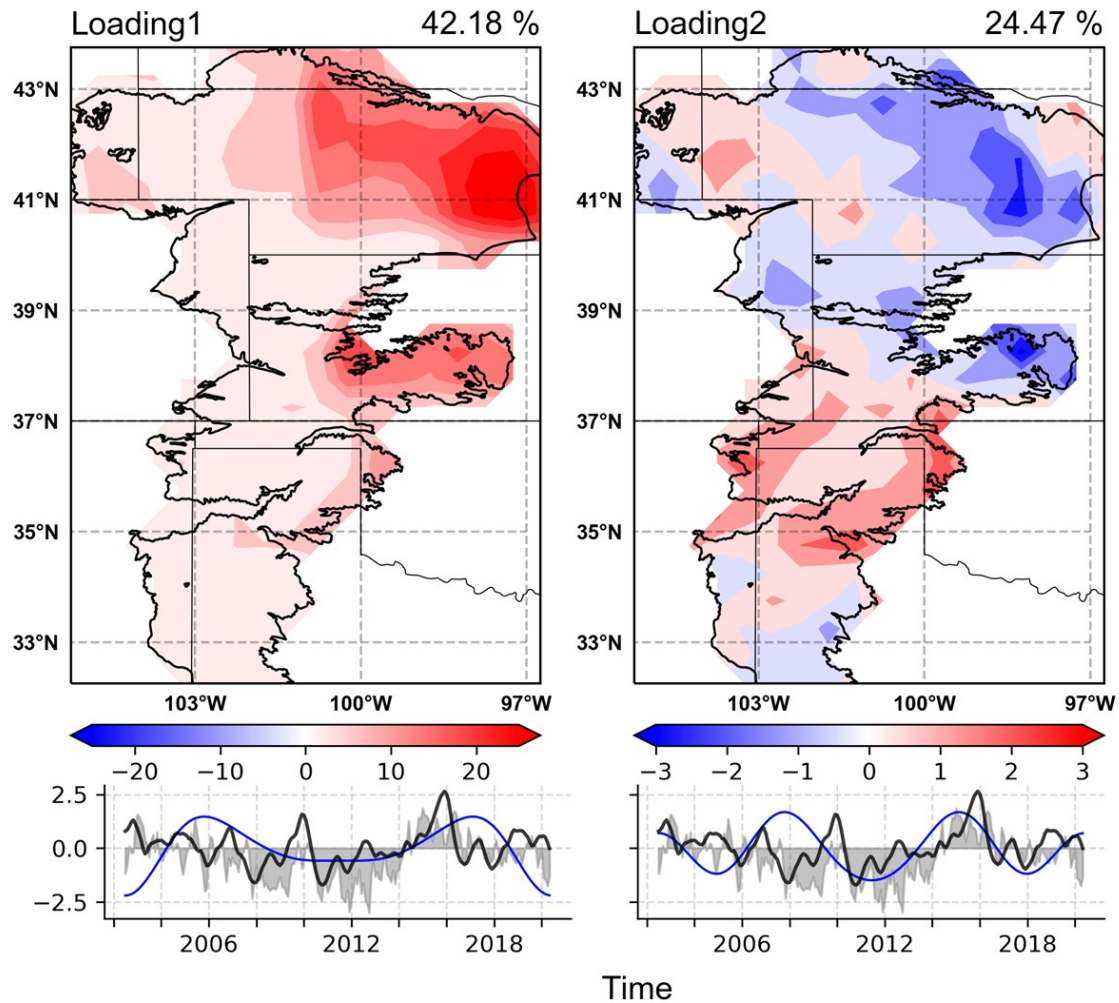
#### Filtering the data with FFT

GWa from well with the longest recording period (KS02 72 years) and GWa derived from GRACE and GRACE-FO were filtered with FFT to observe the variability of the data in the frequencies corresponding to the ENSO and PDO. The annual cycle had more power than the frequencies associated with ENSO but less than the frequencies associated with PDO. The following Figure shows in a) KS02 well, ONI and PDO power spectral density compared. In b) the filtered signal compared with ONI and PDO time series.



After filtering with FFT the GWa derived from GRACE and GRACE-FO, PCA and EOF analysis were performed to observe the resulting modes of variability (Next Figure). The highest variability is concentrated in spring, specifically in May, while in the rest of the seasons the variability is not significant. With the first two components explained 99.5% of the total variance, the first being the most important (97.39%). The first mode affects the northeast (Nebraska and Kansas) and has the same pattern as EOF1, while the second component shows an opposite pattern between the north and south of the aquifer.





The components are influenced by ENSO and PDO, however, to fully capture the variability of the frequencies associated with these components on the High Plains (especially PDO) it is necessary to have longer recording periods.

## CONCLUSIONS

- The northern part of the HPA exhibited increasing water levels while the in central and southern part a decreasing tendency is observed
- In general, the highest water levels are observed in August and the lowest values in March and April. In general, higher values are observed in the Northern High Plains than the southern. It was also observed a spatial increasing gradient from west to east.

- The peak of the monthly values of the wells water levels is approximately 3 months delay with respect to the precipitation peak. This highlighting the temporal lag in the aquifer response from the recharge.
- The northern High Plains is the part with the most variability in the aquifer. This variability is affected more by the annual cycle and PDO than by ENSO.

## AUTHOR INFORMATION

- Juan D. Barrera  
Estudiante de Ingeniería Ambiental, Universidad de Medellín, Colombia.
- Janet Barco  
Facultad de Ingeniería, Ingeniería Ambiental, Universidad de Medellín, Colombia
- Manuela Girotto  
Dept of Environmental Science, Policy & Management, University of California, Berkeley

## ABSTRACT

The Gravity Recovery and Climate Experiment (GRACE) mission and the Follow-On mission (GRACE-FO) have been widely used to estimate Groundwater (GW) at different scales. With improved releases and data longevity of these missions, it becomes possible to analyze changes on GW and its link with global climate patterns such as El Niño-Southern Oscillation (ENSO), which can contribute to better management of this resource, especially in zones where it is crucial for the livelihoods and food security of the community. In the current study, TWS-derived from GRACE, Soil Moisture and Snow simulated by the Global Land Data Assimilation System (GLDAS) were used in the period 2002-2020 to estimate fluctuations in High Plains Aquifer (HPA). Trend and annual cycle were analyzed, and then Principal Component Analysis (PCA) was carry out to observe spatio-temporal oscillation modes and its relationship with Oceanic Niño Index (ONI) through Spectral Analysis. Furthermore, to validate GRACE-derived GW and evaluate a larger period pattern such as Pacific Decadal Oscillation (PDO), Depth to Water data from United States Geological Survey (USGS) wells distributed in the aquifer were selected with a longer period looking for teleconnections.

Results shows increasing trend in Northern High Plains while a decreasing in the central and southern part of it. GW peak occurs in August in most of HPA, three month later than rainfall peak. First four components explain 77% of total variance.

GW derived from GRACE and GRACE-FO as well as GW from wells could detect periodicities that suggest connections of GW variability with PDO more than with ENSO in HPA.

## REFERENCES

Harris, F. (1978). On the Use of Windows for Harmonic Analysis with the Discrete Fourier Transform. *Proceedings of the IEEE*, 66(January), 51–83.

[http://ieeexplore.ieee.org/xpls/abs\\_all.jsp?arnumber=1455106](http://ieeexplore.ieee.org/xpls/abs_all.jsp?arnumber=1455106)

Humphrey, V., & Gudmundsson, L. (2019). GRACE-REC: a reconstruction of climate-driven water storage changes over the last century. *Earth System Science Data Discussions*, 1–41. <https://doi.org/10.5194/essd-2019-25>

Hoerl, A. E., & Kennard, R. W. (1970). Ridge Regression: Biased Estimation for Nonorthogonal Problems. *Technometrics*, 12(1), 55–67.

<https://doi.org/10.1080/00401706.1970.10488634>

Konikow, L. F. (2013). Groundwater Depletion in the United States (1900–2008). *U.S. Geological Survey Scientific Investigations*, 2013–5079, 63.

<https://pubs.usgs.gov/sir/2013/5079/SIR2013-5079.pdf>

Mantua Nathan J., & Hare Steven R. (2002). The pacific decadal oscillation. *Journal of Oceanography*, 58(Figure 23), 35–44

Pandžić, K., & Trninić, D. (1992). Principal component analysis of a river basin discharge and precipitation anomaly fields associated with the global circulation. *Journal of Hydrology*, 132(1–4), 343–360. [https://doi.org/10.1016/0022-1694\(92\)90185-X](https://doi.org/10.1016/0022-1694(92)90185-X)

Rannow, S. (2014). Managing Protected Areas in Central and Eastern Europe Under Climate Change (Vol. 58). <https://doi.org/10.1007/978-94-007-7960-0>

Silva, F. D. F., Fulginiti, L. E., Perrin, R. K., & Schoengold, K. (2019). The Effects of Irrigation and Climate on the High Plains Aquifer : A County-Level Econometric Analysis.